frontiers in Physics

ORIGINAL RESEARCH
published: 23 March 2021
doi: 10.3389/fphy.2021.631471

Thermodynamic Curvature of AdS Black Holes with Dark Energy

*Aditya Singh, Aritra Ghosh and Chandrasekhar Bhamidipati**

School of Basic Sciences, Indian Institute of Technology Bhubaneswar, Odisha, India

In this paper, we study the effect of dark energy on the extended thermodynamic structure and interacting microstructures of black holes in AdS, through an analysis of thermodynamic geometry. Considering various limiting cases of the novel equation of state obtained in charged rotating black holes with quintessence, and taking enthalpy H as the key potential in the extended phase space, we scrutinize the behavior of the Ruppeiner curvature scalar R in the entropy-pressure (S, P)-plane (or equivalently in the temperature-volume (T, V)-plane). Analysis of R empirically reveals that dark energy parameterized by α, significantly alters the dominant interactions of neutral, charged and slowly rotating black hole microstructures. In the Schwarzschild-AdS case: black holes smaller than a certain size continue to have attractive interactions whereas larger black holes are completely dominated by repulsive interactions which arise to due dark energy. For charged or rotating AdS black holes with quintessence, R can change sign at multiple points depending upon the relation between α and charge q or angular momentum J. In particular, above a threshold value of α, R is never negative at all, suggesting heuristically that the repulsive interactions due to quintessence are long ranged as opposed to the previously known short ranged repulsion in charged AdS black holes. A mean field interaction potential is proposed whose extrema effectively capture the points where the curvature R changes sign.

Keywords: black holes, thermodynamic geometry, anti de Sitter space, thermodynamics, quantum gravity

OPEN ACCESS

Edited by:
Oscar Dias,
University of Southampton,
United Kingdom

Reviewed by:
George Ruppeiner,
New College of Florida, United States
Jennie Traschen,
University of Massachusetts Amherst,
United States

****Correspondence:***
Chandrasekhar Bhamidipati
chandrasekhar@iitbbs.ac.in

Specialty section:
This article was submitted to High-Energy and Astroparticle Physics, a section of the journal Frontiers in Physics

Received: *20 November 2020*
Accepted: *25 January 2021*
Published: *23 March 2021*

Citation:
Singh A, Ghosh A and Bhamidipati C (2021) Thermodynamic Curvature of AdS Black Holes with Dark Energy. Front. Phys. 9:631471. doi: 10.3389/fphy.2021.631471

1 INTRODUCTION

Cosmological data points toward an accelerated expansion of our Universe due to the presence of a large negative pressure leading to the conjectured existence of an anti-gravitational force, namely dark energy [1–3]. Despite the prevalence of several theoretical models in efforts to explain astronomical observations, the key traits of dark energy such as its source and nature still remain mysterious. Some of the models for dark energy employ a cosmological constant Λ or a quintessence field. Λ is a very small constant whereas quintessence energy is quite inhomogeneous. Quintessence can be thought of as a fluid that fills the spacetime everywhere [4–6] and is modeled as a time dependent scalar field $\phi(t)$ evolving toward its potential minimum. It is associated with pressure, $P_q = \dot{\phi}^2/2 - U(\phi)$ and energy density, $\rho_q = \dot{\phi}^2/2 + U(\phi)$ where $U(\phi)$ is the potential function. Often, it is useful to define a quintessential state parameter as, $\omega_q = P_q/\rho_q$ and it is clear that in general $\omega_q \in (-1, 1)$ with the extreme limits corresponding respectively to $\dot{\phi} \to 0$ and $U(\phi) \to 0$. It is generally believed that the late time evolution is because of the cosmological constant or quintessence field permeating through the Universe. Therefore, if the quintessence fluid encompasses the whole Universe, it is expected to also surround the black holes changing their

spacetime geometry both near the horizon as well as at the asymptotic cosmological horizon. In this context, a new spherically symmetric quintessence black hole solutions were found in $(3+1)$-dimensions by Kiselev [7] and the solution in AdS space time is well studied in the literature from thermodynamics point of view [8–14]. Here, we should caution the reader about the usage of the terminology of quintessence in Kiselev's black hole metric which may be different from the notion used in cosmology modeled by a scalar field as discussed above. Few reasons follow. First, Kiselev's metric may not be a solution of field equations derived from a gravitational action coupled to specified matter Lagrangian (such as representing quintessence field). Instead, the form of energy-momentum tensor in Kiselev's approach is a specific choice with free parameters, picked in a way to give features of quintessence and inserted in to the field equations. Furthermore, the stress-energy tensor used in the Kiselev's metric is anisotropic and does not represent a perfect fluid. Therefore, our usage of the terminology of quintessence in Kiselev black hole spacetimes considered in this paper is within the limitations of these conditions (please see [15] for more clarity on these issues). Despite these limitations, Kiselev's quintessence black hole metric is an interesting toy model, as being spacetimes which can be explored, with some appealing mathematical as well as physical features. For special limiting values of the equation of state parameter (to be discussed later) the pure quintessence geometry without mass or charge/rotation parameters can model spacetimes with asymptotic geometry which is a softer version of de Sitter or anti de Sitter spacetimes [16] and is of interest. We also see in this paper that the additional contribution due to quintessence helps in developing our understanding of the behavior of black hole microstructues in a broader setting with additional parameters.

An interesting aspect of black hole thermodynamics ensues while generalizing the notion of ADM mass from asymptotically flat to (A) dS spacetimes, namely the requirement of a dynamical cosmological constant. A variable Λ plays a central role in extending Smarr's formula from flat to AdS spacetimes, typically giving rise to the notion of bulk pressure P and a novel concept of thermodynamic volume V [17, 18]. This novel set up where the first law is augmented by a VdP term coming from a dynamical Λ is known as extended black hole thermodynamics [19–21]. In this approach, the ADM mass M of the spacetime is identified with its enthalpy (rather than internal energy U) as $M = H = U + PV$, with the new first law being written as,

$$\mathrm{d}H = T\mathrm{d}S + V\mathrm{d}P, \tag{1}$$

where $V = (\partial H/\partial P)_S$ is the thermodynamic volume conjugate to P. For charged black holes, there turns out to be an exact identification of its phase transitions [19, 22, 23] (including the matching of critical exponents) with the well known liquid-gas transitions of a van der Waals fluid (vdW) [24], putting them in the same universality class [24–29]. Thermodynamic quantities of charged rotating black holes in AdS in extended phase space were found by Gunasekaran et al. in [30]. Results were extended to Gauss-Bonnet-AdS black holes by Cai et al. and Wei et al. in [25, 31]. All the above set ups have also been generalized to black holes in AdS with quintessence in interesting works. For instance, effects of quintessence on the PV-critical behavior of charged AdS black holes was worked out in [32] showing that the critical quantities are modified, but the small/large black hole behavior remains the same. Further, the effect of dark energy on the efficiency of black hole heat engines has been studied in [33] showing that quintessence can improve the efficiency, especially at the critical point. Maxwell's equal area law was used by Guo in [34] to show that phase transitions of AdS black holes with quintessence can still be mapped to those of the liquid-gas system. More recently, it has been shown that quintessence alters the high temperature phase structure of black holes undergoing the Hawking-Page transition [35]. In fact, a novel black hole solution of charged rotating black holes in AdS in the presence of quintessence, generalizing the Kiselev's metric was obtained by Xu and Wang [36]. For this new solution, the thermodynamics and phase transitions in the extended thermodynamic space were discussed recently giving rise to a novel equation of state [37]. Our aim is to take these studies [36, 37] forward to study the geometry of the spaces of thermodynamic equilibrium states for these black hole solutions and to get additional insights into the possible microstructures of these black holes.

The fact that a black hole horizon can be assigned the notion of a temperature indicates toward a microscopic description of black holes where microstructures share the degrees of freedom of the Bekenstein-Hawking entropy [38–42]. These microscopic structures have associated with them, thermal degrees of freedom and respect equipartition theorems (see for example [43]). With this picture in mind, it is useful to think of the microstructures of the black hole in parallel with the molecules that constitute a fluid system in standard thermodynamics and the study of thermodynamic geometry proves to be of outmost importance in its usefulness in probing the nature of interactions between the microstructures [44–73]. To the best of our knowledge, Ruppeiner geometry for black holes was first used in [44], to gain a statistical understanding of the underlying degrees of freedom, with extensions to Reissner-Nordström, Kerr and Reissner-Nordström-AdS black holes with internal energy and electric potential (or angular velocity for Kerr black hole case) as the fluctuation variables [47]. For example, based on empirical analysis, it is now known that charged AdS black holes are associated with both attraction and repulsion dominated regions as shown in remarkable works [62, 63]. Extending to theories with higher derivative terms, including those with a Gauss-Bonnet term in the action, the attraction-repulsion dominated regions are determined by their electric charge (and Gauss-Bonnet coupling, α_{GB} in $\mathrm{d} \geq 6$) whereas, their neutral counterparts are dominated by attraction [66–69]. Charged BTZ black holes (see [73] and references therein) on the other hand, are associated with purely repulsive behavior. More recently, Ruppeiner geometry has given intriguing results for charged black holes with spherical [70] and hyperbolic horizons [72], with deep insights in Hawking-Page transition and Renormalization group (RG) flows, respectively. The effect of quintessence (along with a cloud of strings) on phase transitions

of charged black holes in AdS was pursued in [14, 58] recently. In general, thermodynamic geometry [74] and its generalizations have been the subject of various exhaustive studies involving several classes of thermodynamic systems including quantum gases, magnetic systems [75–78] (see also [79–81]) and most notably black holes. The generic form of the Ruppeiner metric is defined as the negative Hessian of the entropy,

$$\mathrm{d}l_R^2 = -\frac{\partial^2 S}{\partial x^i \partial x^j}\mathrm{d}x^i \mathrm{d}x^j, \tag{2}$$

where x^i and x^j are independent thermodynamic fluctuation coordinates $i, j \in \{1, 2, \ldots, n\}$. The entropy $S = S(x^i)$ is a function of other thermodynamical variables and the coordinates x^i are conserved charges of the black holes such as M, Q, J and also span over the new variable P, V in extended thermodynamics. For example, in the case of Schwarzschild-AdS black holes one has $S = S(H, P)$ where symbols have their usual meaning from standard thermodynamics. This may be inverted to obtain $H = H(S, P)$ so that in the thermodynamic limit, one has the familiar first law[1]: $\mathrm{d}H = T\mathrm{d}S + V\mathrm{d}P$. In fact, one can write another related Weinhold metric on the space of thermodynamic equilibrium states in the enthalpy $H = M$ representation[2] as

$$\mathrm{d}l_W^2 = \frac{\partial^2 H}{\partial y^i \partial y^j}\mathrm{d}y^i \mathrm{d}y^j \tag{3}$$

where $\{y^i\}$ are independent thermodynamic variables, such as (S, P). It is not difficult to show that $\mathrm{d}l_R^2 = \mathrm{d}l_W^2/T$ and therefore the metrics differ only by a conformal factor (please see **Supplementary Appendix** for a concise derivation).

Motivation and plan: In this work, thermodynamic geometry is pursued in extended thermodynamics where enthalpy in **Eq. 1** is identified as the correct thermodynamic potential [17] for the proper identification of microstructure interactions with quintessence, keeping the vdW analogy in mind. Using enthalpy as the key potential, the effect of dark energy on microstructures using thermodynamic geometry is appropriately studied in (T, V) and (S, P)-planes, following references [62–73]. We consider various limiting cases arising from the novel equation of state obtained recently in [37] and use Ruppeiner's thermodynamic geometry to show that the inclusion of quintessence leads to novel repulsion dominated regions, modifying the behavior of microstructures of neutral, charged and rotating black holes in AdS. Furthermore, we introduce a phenomenological model of a mean field interaction potential for the analysis in the extended thermodynamics setting where a direct analogy with fluid systems is available. It is shown that the extrema of the interaction potential correspond to the points where the Ruppeiner curvature is zero, essentially capturing the location where the type of dynamic interactions shift from attractive to repulsive or vice-versa. The organization of the paper is as follows. In **Section 1.1** below, we start by writing down the thermodynamic relations for general charged rotating black holes in AdS surrounded by quintessence field. **Section 2** contains the basic tools of Ruppeiner geometry required to find the thermodynamic curvature. The metric on thermodynamic space in the novel (T, V)- and (S, P)-planes is obtained and a general formula for Ruppeiner curvature is reviewed. In **Section 3** we obtain exact results for thermodynamic curvature and study the points where it vanishes for the special cases of Reissner-Nordström and Schwarzschild black holes in AdS, surrounded by quintessence. The case of slowly rotating black holes with quintessence is studied numerically in following section. In **Section 4**, we propose a general scheme for understanding the behavior of microstructures of AdS black holes from a mean field perspective, which in particular, captures the points where the Ruppeiner curvature vanishes. The case of charged AdS black holes (without quintessence) is discussed first in **Section 4.1** and then in **Section 4.2**, we discuss the effect of quintessence on the microstructures of charged and neutral black holes in AdS using the interaction potential. Finally, we end with remarks in **Section 5**. Some introductory discussions on thermodynamic metric structures, particularly in the context of extended black hole thermodynamics can be found in the **Supplementary Appendix**.

1.1 Thermodynamics of AdS Kerr-Newman Black Holes Surrounded by Dark Energy

Making use of Newman-Penrose formalism [83], the solution for a Kerr-Newman-AdS black hole generalizing the Kiselev's model metric with quintessence, was obtained by Xu and Wang [36], with the line-element in Boyer-Lindquist coordinates given as,

$$\begin{aligned}\mathrm{d}s^2 = &-\frac{\chi}{\Omega}\left[\mathrm{d}t - \frac{a\sin^2\theta}{k}\mathrm{d}\phi\right]^2 + \frac{\Omega}{\chi}\mathrm{d}r^2 + \frac{\Omega}{\tilde{P}}\mathrm{d}\theta^2 \\ &+ \frac{\tilde{P}\sin^2\theta}{\Omega}\left[a\mathrm{d}t - \frac{(r^2+a^2)}{k}\mathrm{d}\phi\right]^2.\end{aligned} \tag{4}$$

Here,

$$\chi = \left(r^2 + a^2\right)\left(1 + \frac{r^2}{l^2}\right) - 2mr + q^2 - \alpha r^{1-3\omega_q}, \tag{5}$$

$$\Omega = r^2 + a^2\cos^2\theta, \quad k = 1 - \frac{a^2}{l^2}, \quad \tilde{P} = 1 - \frac{a^2}{l^2}\cos^2\theta, \tag{6}$$

where a is the rotation parameter and $q^2 = q_e^2 + q_m^2$ with q_e and q_m being the electric and magnetic charges respectively. Further, m is the black hole mass and $l = \sqrt{-3/\Lambda}$ is the AdS radius. In general, the state parameter ω_q is bounded as $-1 < \omega_q < -\frac{1}{3}$ and α is the parameter standing for the intensity of the quintessential field surrounding a black hole, obeying the inequality [36],

[1]For a rotating black hole one can write the first law as: $\mathrm{d}H = T\mathrm{d}S + V\mathrm{d}P + \Phi\mathrm{d}Q + \Omega\mathrm{d}J$ (in the usual notation) where $H = U + PV$ is the enthalpy of the spacetime pointing toward the fact that the entropy is a function of the parameters, i.e., $S = S(H, Q, J, P)$. However, for simplicity we shall completely fix J and Q as mere parameters and consider fluctuations of two thermodynamic variables only.

[2]The Weinhold metric is originally defined in the energy representation [82], taking U as the key potential. In standard black hole thermodynamics U is identified with mass M of the black hole to evaluate the metric on the space of thermodynamic equilibrium states. However, in extended thermodynamics M is identified with enthalpy H and hence it is appropriate to call it an enthalpy representation.

$$\alpha \leq \frac{2}{1-3\omega_q} 8^{\omega_q}. \tag{7}$$

Quintessence has been introduced as an alternative to the cosmological constant scenario to account for the current acceleration of the Universe. This new dark energy component allows values of the equation of state parameter $\omega_q \geq -1$. The case of a cosmological constant corresponds to the value $\omega_q = -1$. Kiselev [7] noted that the value of $\omega_q = -2/3$ is favorable on symmetry grounds (the general metric is symmetric as function of radial coordinate r), in addition to having an asymptotic behavior reminiscent of de Sitter spacetimes with interesting horizon structure. Moreover, this case also satisfies the dominant energy condition [16, 84]. The analysis of PV-criticality and other studies in charged AdS black holes surrounded by quintessence [32, 33] showed that another appealing feature is that analytic results could be obtained for this value, where as for other values, one has to resort to numerical methods. We thus focus on the case $\omega_q = -2/3$ henceforth, which allows an analytic study of the mean field potential and its connection to zeroes of Ruppeiner scalar in following sections. Note that for $\alpha = 0$, the line element **(4)** reduces to the Kerr-Newman-AdS solution while the Kerr-AdS solution can be obtained by further setting $q = 0$. We explore these and other limits in subsequent sections.

Useful expressions for mass, entropy and temperature are given respectively as,

$$m = \frac{1}{2r_+}\left(r_+\left(\frac{r_+\left(a^2+l^2+r_+^2\right)}{l^2} - \alpha r_+^2\right) + a^2 + q^2\right), \tag{8}$$

$$S = \frac{A}{4} = \frac{\pi\left(a^2+r_+^2\right)}{k}, \tag{9}$$

$$T = \frac{1}{4\pi\left(a^2+r_+^2\right)}\left(2\left(\frac{r_+\left(a^2+l^2+2r_+^2\right)}{l^2} - m\right) - 3\alpha r_+^2\right). \tag{10}$$

In extended black hole thermodynamics, the cosmological constant is identified with pressure as,

$$P = -\frac{\Lambda}{8\pi} = \frac{3}{8\pi l^2}, \tag{11}$$

with its thermodynamic conjugate volume obtained as,

$$V = \left(\frac{\partial M}{\partial P}\right)_{S,Q,J,\alpha} = \frac{2\pi\left(a^2l^2\left(q^2-\alpha r_+^3\right) + \left(a^2+r_+^2\right)\left(a^2l^2 - a^2r_+^2 + 2l^2r_+^2\right)\right)}{3k^2l^2r_+}. \tag{12}$$

Here mass M, angular momentum J and charge Q, are related to parameters m, a and q as follows,

$$M = \frac{m}{k^2}, \quad J = \frac{ma}{k^2}, \quad Q = \frac{q}{k}. \tag{13}$$

The physical parameters M, J and Q now satisfy the Smarr-Gibbs-Duhem relation [37],

$$M = 2\left(TS - PV + \Pi J\right) + Q\Phi + \alpha\Psi\left(-\frac{2a^2}{a^2+r_+^2} - 1\right), \tag{14}$$

where the electric potential Φ and Ψ (which is conjugate to α) [32] are given as,

$$\Phi = \frac{qr_+}{a^2+r_+^2}, \quad \Psi = -\frac{r_+^2}{2k}. \tag{15}$$

Let us note that when $\alpha = 0$, all the above quantities go back to the relations for charged rotating AdS black holes [30]. The Hawking temperature in terms of pressure can be written as [37],

$$T = \frac{2r_+\left(8\pi P\left(a^2+2r_+^2\right)+3\right) - r_+\left(8\pi a^2P+3\right) - \frac{3\left(a^2+q^2\right)}{r_+} - 8\pi Pr_+^3 - 6\alpha r_+^2}{12\pi\left(a^2+r_+^2\right)}. \tag{16}$$

The plot of temperature vs volume is shown in **Figure 1**.

The above equation needs to be inverted to obtain the equation of state of the general Kerr-Newman AdS black holes. However, as noted in [30], it is in general not possible to obtain an exact expression and hence one resorts to the slowly rotating charged black hole case, where the equation of state is [37],

$$P = \frac{T}{2r_+} + \frac{Q^2}{8\pi r_+^4} - \frac{1}{8\pi r_+^2} + \frac{\alpha}{4\pi r_+} + \frac{3J^2\left(Q^2r_+^2 - 2Q^4 - 8\pi Q^2r_+^3T - 4\alpha Q^2r_+^3 + 8\pi r_+^5T - 2\alpha r_+^5 + 4r_+^4\right)}{8\pi r_+^6\left(2Q^2 + 2\pi r_+^3T - \frac{1}{2}\alpha r_+^3 + r_+^2\right)^2} + O\left(J^4\right), \tag{17}$$

which is an expansion in powers of J and terms of order $O(J^4)$ are neglected in further analysis. In the following sections, various limiting cases of the above equation of state are considered leading to neutral, charged and (slowly) rotating black holes in AdS with quintessence. For each of the cases, the behavior of thermodynamic curvature is studied and for the former two cases, a mean field potential description is also obtained.

2 RUPPEINER GEOMETRY AND MICROSCOPIC INTERACTIONS

To begin with, consider a thermodynamic system with some n independent thermodynamic variables which can fluctuate about their mean values. A prototypical example with $n = 2$ would be a hydrostatic system with a fixed volume described by the grand canonical ensemble. The external bath controls the temperature (β) and chemical potential (μ) of the system whereas their respective thermodynamic conjugates, namely energy[3] and number of particles are allowed to have fluctuations about their mean values. If the system is at equilibrium, which we shall assume throughout this work, the first derivatives of the entropy shall vanish identically which means that expanding S

[3]Typically, temperature is conjugate to the entropy as is clear from the first law, $dE = TdS +$ other terms. However, inverting this and writing as, $dS = \beta dE + \ldots$, leads to the notion of β being conjugate to energy.

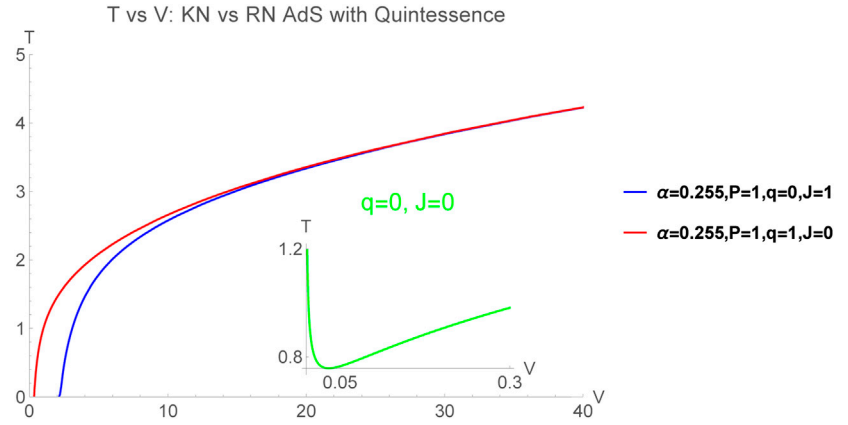

FIGURE 1 | Plot of the Hawking temperature vs thermodynamic volume.

about its equilibrium value S_0 to include effects of fluctuations one can write up to the lowest non-trivial order,

$$S \approx S_0 + \frac{\partial^2 S}{\partial x^i \partial x^j} \mathrm{d}x^i \mathrm{d}x^j, \tag{18}$$

where $\{x^i\}$ are the fluctuation coordinates the entropy is a function of, and $i = 1, 2 \ldots . n$. It is understood that the derivatives are evaluated at thermodynamic equilibrium. Recalling Boltzmann's definition of entropy as a measure of the probability as $S = \ln \Omega$, one can invert this, writing $\Omega = e^S$ and then the probability of finding the system with the independent variables between x^i and $x^i + \mathrm{d}x^i$ for all i is then given by,

$$P \mathrm{d}x^1 \mathrm{d}x^2 \ldots . \mathrm{d}x^n = C e^{-\mathrm{d}l_R^2} \mathrm{d}x^1 \mathrm{d}x^2 \ldots . \mathrm{d}x^n, \tag{19}$$

where we have used **Eq. 18** and have written,

$$\mathrm{d}l_R^2 = -\frac{\partial^2 S}{\partial x^i \partial x^j} \mathrm{d}x^i \mathrm{d}x^j, \tag{20}$$

Clearly, **Eq. 20** defines a length element on the space of independent thermodynamic variables describing the system. However, such a length has great physical meaning. Indeed, from **Eq. 19** it is clear that for any two points on the space of independent thermodynamic variables, the probability of them being related by a fluctuation more, the closer they are! The reader is referred to [79–81] for a much more detailed account on the role of the Ruppeiner metric in thermodynamic fluctuation theory. Note that taking any arbitrary thermodynamic potential, $\phi = \phi(z^i)$ with new coordinates z^i, one can define a metric as follows,

$$\mathrm{d}l^2 = -\frac{\partial^2 \phi}{\partial z^i \partial z^j} \mathrm{d}z^i \mathrm{d}z^j. \tag{21}$$

This would still in some sense define a length between different thermodynamic equilibrium states. However, in general it may not have a good connection with thermodynamic fluctuation theory and may not result in curvature scalar with nice interpretation (like the one provided by Ruppeiner scalar R) as the measure of interactions of the system. The metric in **Eq. 21** may be meaningful if it is obtained from **Eq. 20** by an appropriate coordinate transformation. More details are given in the **Supplementary Appendix**.

2.1 Line Element and Ruppeiner Curvature

To proceed with the study of thermodynamic geometry of the black holes in AdS with quintessence background, we note that even though the Ruppeiner metric [**Eq. 2**] is initially defined as the Hessian of the entropy, one can calculate equivalent forms of the metric using other potentials such as the enthalpy, $H = H(S, P)$ in **Eq. 27**, where the fluctuation coordinates are simply S and P. We shall, in this work, study Ruppeiner geometry on the (T, V)- and (S, P)-planes, i.e., using both enthalpy and Helmholtz free energy representations[4]. The line element on the (S, P)-plane can be calculated without much difficulty and reads [66, 68] (see **Supplementary Appendix** for derivation),

$$\mathrm{d}l_R^2 = \frac{1}{C_P} \mathrm{d}S^2 + \frac{2}{T} \left(\frac{\partial T}{\partial P} \right)_S \mathrm{d}S \mathrm{d}P - \frac{V}{T B_S} \mathrm{d}P^2, \tag{22}$$

where $B_S = -V(\partial P / \partial V)_S$ is the adiabatic bulk modulus which diverges for non-rotating black holes (in $\mathrm{d} \geq 4$) obtained by setting $J = 0$ wherein, the entropy and volume are not independent. Similarly, the Ruppeiner line element on the (T, V)-plane is given by [66,68],

$$\mathrm{d}l_R^2 = \frac{1}{T} \left(\frac{\partial P}{\partial V} \right)_T \mathrm{d}V^2 + \frac{2}{T} \left(\frac{\partial P}{\partial T} \right)_V \mathrm{d}T \mathrm{d}V + \frac{C_V}{T^2} \mathrm{d}T^2, \tag{23}$$

where C_V is the specific heat at constant volume which is zero for black holes where the geometric volume coincides with the thermodynamic volume. In four or more dimensions, this is true for all static (non-rotating) black holes. Since we consider the

[4]As also pointed out in [66], an internal energy representation, i.e., the (S, V)-plane is not suitable for many black hole systems where the fluctuation coordinates S and V are not independent.

slowly rotating black hole approximation, C_V shall still be taken to be zero. A derivation of these line elements is presented at the end in the **Supplementary Appendix**.

Now that it is understood that the Ruppeiner metric defines a physically meaningful distance on the spaces of thermodynamic equilibrium states, let us go further and analyze the meaning of the corresponding Ricci scalar. For a two dimensional metric, i.e., with two fluctuation coordinates as we shall be using in this work, the components of the metric can be written down as a 2×2 matrix, g_{ij} with $i = 1, 2$. The Ricci scalar of the geometry described by the Ruppeiner metric can be calculated by the rules of Riemannian geometry. This Ricci scalar shall be called the Ruppeiner curvature and contains the physical information of the microscopic interactions in a thermodynamic system. For such a metric, the Ricci scalar can be written down as (see for example [81]),

$$R = -\frac{1}{\sqrt{g}}\left[\frac{\partial}{\partial x^1}\left(\frac{g_{12}}{g_{11}\sqrt{g}}\frac{\partial g_{11}}{\partial x^2} - \frac{1}{\sqrt{g}}\frac{\partial g_{22}}{\partial x^1}\right) + \frac{\partial}{\partial x^2}\left(\frac{2}{\sqrt{g}}\frac{\partial g_{12}}{\partial x^1} - \frac{1}{\sqrt{g}}\frac{\partial g_{11}}{\partial x^2} - \frac{g_{12}}{g_{11}\sqrt{g}}\frac{\partial g_{11}}{\partial x^1}\right)\right], \tag{24}$$

where $g = g_{11}g_{22} - g_{12}g_{21}$ is the determinant of the 2×2 matrix g_{ij}. The Ruppeiner curvature calculated for any set of fluctuation coordinates for the classical ideal gas identically comes out to be zero whereas that for the vdW fluid comes out to be negative over the entire physical region[5] At the first instance, it appears that the Ruppeiner curvature may indicate whether interactions are present in the system. If instead, one looks at ideal quantum gases like the ideal Bose or the ideal Fermi gas, by virtue of being "ideal" such gases are expected to be weakly interacting like the classical ideal gas meaning that the only interactions between particles can be the collisions. However, computation of the Ruppeiner curvature for ideal Bose and Fermi gases give opposite signs [78]. In the sign convention adopted in this work (opposite to that of [78]), the ideal Bose gas is associated with a Ruppeiner curvature which always carries a negative sign whereas, that for the Fermi gas carries a positive sign. It is known that fermions typically have repulsive interactions of quantum mechanical origin between them as a direct consequence of the exclusion principle which leads to the familiar notion of a Fermi pressure. The Ruppeiner curvature being negative definite for an attractive vdW fluid and being positive definite for a repulsive quantum gas of fermions strongly suggests its relationship with the nature of interactions between the underlying degrees of freedom of the system. Further, an ideal gas of bosons has with it associated a negative definite thermodynamic curvature which is also consistent with the fact that bosons tend to come closer to each other, an interaction which is yet again of purely quantum mechanical origin. The Ruppeiner curvature therefore, not only probes the vdW type interactions, but also interactions arising out of the quantum mechanical nature of the underlying degrees of freedom and as such, it is a perfect macroscopic probe which may be used to understand how the microscopic constituents of a given thermodynamic system interact [79–81] (see also [85]). This deserves special attention for the case of black holes where a microscopic theory is not well understood and hence, Ruppeiner geometry is expected to provide us with early microscopic insights.

[5]See for example the recent work [63] where the Ruppeiner curvature of the vdW fluid in the novel (T, V)-plane has been presented.

3 EFFECT OF DARK ENERGY ON THERMODYNAMIC GEOMETRY

From the form of the equation of state given in **Eq. 17**, it is helpful to first discuss the thermodynamic geometry of cases $J = 0, \quad Q = 0$ and $J = 0, \quad Q \neq 0$, corresponding to neutral and charged black holes in AdS, respectively surrounded by quintessence, where an exact analysis is possible. In these case, it is also possible to explicitly see the form of mean field potential (**Section 4**). The other case of interest, i.e., $Q = 0, \quad J \neq 0$ is discussed in **Section 3.2**, separately as the expressions for thermodynamic curvature are quite involved and the behavior can only be studied numerically.

3.1 Schwarzschild and Reissner-Nordström Black Holes in AdS

Setting the rotation parameter in **Eq. 4** to zero, we get a Reissner-Nordström-AdS (RN-AdS) black hole surrounded by quintessence, whose lapse function $f(r)$ takes the form [7],

$$f(r) = 1 - \frac{m}{r} + \frac{q^2}{r^2} + \frac{r^2}{l^2} - \alpha r, \tag{25}$$

$$F = \mathrm{d}A, \quad A = -\frac{q}{r}\mathrm{d}t. \tag{26}$$

Making the usual identification that the ADM mass of the black hole and expressing it as function of entropy and pressure, one gets enthalpy to be,

$$H(S, P) = \frac{1}{2}\sqrt{\frac{S}{\pi}}\left(1 + \frac{\pi q^2}{S} - \alpha\left(\sqrt{\frac{S}{\pi}}\right) + \frac{8PS}{3}\right). \tag{27}$$

Note that in this non-rotating case, one has $Q = q$. Thermodynamic volume can now be obtained from $V = (\partial H/\partial P)_{S,q,\alpha}$ as,

$$V = \frac{4\pi r_+^3}{3}, \tag{28}$$

and is found to be same as geometric volume [33]. With all definitions of fundamental thermodynamic variables available, the first law of black holes in the extended thermodynamic phase space can be written to be,

$$\mathrm{d}M = \mathrm{d}H = T\mathrm{d}S + \Phi\mathrm{d}q + V\mathrm{d}P + \psi\mathrm{d}\alpha, \tag{29}$$

where $\Phi = (\partial H/\partial q)_{S,P,\alpha}$ is the electric potential conjugate to charge q and $\psi = (\partial H/\partial \alpha)_{S,q,P}$ is a quantity conjugate to the parameter α. It should be mentioned that the first law given in **Eq. 29** is phenomenological, which makes the first law and Smarr

relation consistent [33]. A full derivation would require the use of field equations extending the techniques used in [17] to the current situation involving quintessence. We will work in the canonical ensemble where $dq = d\alpha = 0$. The Hawking temperature [**Eq. 29**] takes a simplified form,

$$T = \frac{1}{4\pi}\left(\frac{1}{r_+} - \frac{q^2}{r_+^3} - 2\alpha + 8\pi P r_+\right). \tag{30}$$

Further, setting $J = 0$ in **Eq. 17** and identifying the specific volume to be $v = 2r_+$, one obtains the standard fluid-like equation of state $P = P(v, T)$,

$$P = \frac{T}{v} + \frac{\alpha}{2\pi v} - \frac{1}{2\pi v^2} + \frac{2q^2}{\pi v^4}, \tag{31}$$

which corresponds to that of a non-ideal fluid, i.e., one with non-trivial interactions between molecules. Each of the last three terms in **Eq. 31** signify interactions between the microstructures. The limit $\alpha = 0$ gives the well known equation of state for standard RN-AdS black holes in $(3+1)$-dimensions [24]. Using the above equations for temperature and equation of state, the line elements in **Eqs. 22**,**23** can be obtained. For instance, the 2×2 metric tensor on the (S, P)-plane turns out to be,

$$g_{ij} = \begin{pmatrix} \frac{\sqrt{\pi}(3\pi q^2 + S(8PS-1))}{2S(\sqrt{\pi}(-\pi q^2 + 8PS^2 + S) - 2S^{3/2}\alpha)} & \frac{8\sqrt{\pi}S^2}{\sqrt{\pi}(-\pi q^2 + 8PS^2 + S) - 2S^{3/2}\alpha} \\ \frac{8\sqrt{\pi}S^2}{\sqrt{\pi}(-\pi q^2 + 8PS^2 + S) - 2S^{3/2}\alpha} & 0 \end{pmatrix} \tag{32}$$

where $i, j = S, P$. We can now give the analytical expressions of the Ruppeiner curvature for RN-AdS black holes surrounded by quintessence in the background, both on (S, P) and (T, V)-planes respectively as,

$$R_{SP} = -\frac{\sqrt{\pi}(2\pi q^2 - S) + S^{3/2}\alpha}{\sqrt{\pi}S(\pi q^2 - S(1 + 8PS)) + 2S^{5/2}\alpha}, \tag{33}$$

and

$$R_{TV} = \frac{8\pi q^2 - 6^{2/3}\pi^{1/3}V^{2/3} + 3V\alpha}{3 \times 6^{2/3}\pi^{4/3}TV^{5/3}}. \tag{34}$$

It should be noted that both R_{SP} and R_{TV} asymptotically diverge as the black hole becomes extremal, i.e., $T = 0$. The scalar R_{SP} is plotted in **Figure 2** (as a function of S for fixed P. The scalar R_{TV} shows identical behavior and is plotted in **Figure 3**.

On either of the thermodynamic planes, it is found that the Ruppeiner curvature admits zero crossings indicating existence of points where the dominant kind of interactions can switch from attractive to repulsive and vice versa, since the sign of the Ruppeiner curvature indicates the nature of microscopic interactions. Let us first note that for $\alpha = 0$, both R_{SP} and R_{TV} reduce to the previous expressions for the RN-AdS black hole obtained in [68]. Furthermore, the curvature scalars given in **Eqs. 33**,**34** can be checked to be equivalent so we may label them as R. Second, for a given value of charge q, there is a possibility that for a value of α, the Ruppeiner curvature changes sign twice. The points where $R = 0$ occur at $S =$ 13.8, 27.8 for the value $\alpha = 0.26$, $q = 1$ in **Figure 2**. This is to be contrasted with the situation for RN AdS black holes with no quintessence [62, 63, 68], where there is only one point where the Ruppeiner curvature crosses from repulsive to attractive type interactions of microstructures (plot for RN-AdS black holes is given as an inset in **Figure 2**). The condition $R = 0$ occurs at points which are the physical solutions to the algebraic equation,

$$2\pi^{3/2}q^2 + \alpha S^{3/2} - \sqrt{\pi}S = 0. \tag{35}$$

The crossing points therefore depend on the parameters α and q of the black hole. A plot of S vs α shown in **Figure 4** gives interesting insights.

As seen from **Figure 4** the number of zero crossing points are either zero, one or two depending for a particular case on how many real solutions **Eq. 35** admits based on the values of α and q. As mentioned above, the existence of one zero of the Ruppeiner

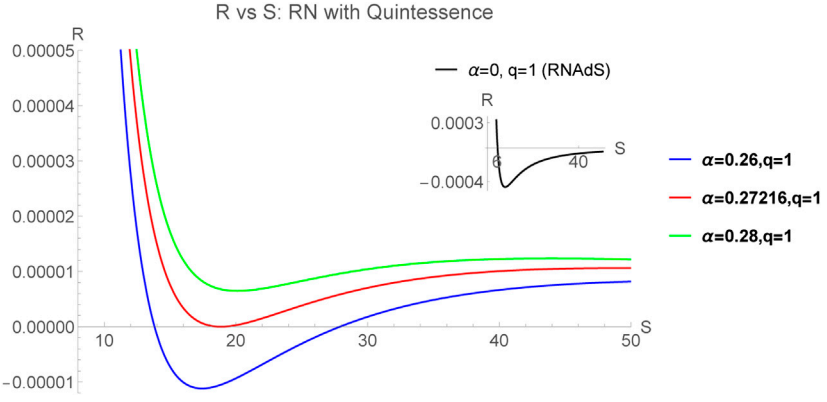

FIGURE 2 | Ruppeiner curvature on the (S,P)-plane as a function of S for fixed P.

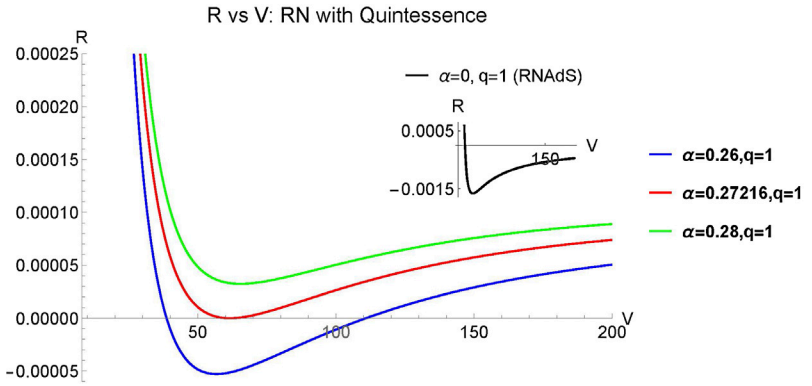

FIGURE 3 | Ruppeiner curvature on the (T,V) plane as a function of V for fixed T.

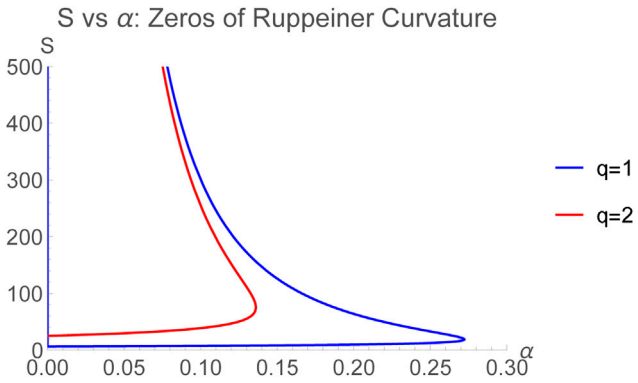

FIGURE 4 | Points in the parameter space where the Ruppeiner Curvature is flat.

curvature at small value of S[6] at which the attractive and repulsive interactions balance each other is well known for the RN-AdS system [68]. The cases where there's a second zero (see **Figure 2**) at a higher entropy (or equivalently horizon size), are new and of particular interest here, because they are associated with the presence of quintessence in the background. In fact, there are two further remarkable results. First is the existence of a point on the S-axis (the red curve in **Figure 2**) corresponding to a threshold value of $\alpha = \alpha_0$ (depending on q), where the R starts out positive, barely vanishes at a value of S and continues to be positive after that. This threshold value occurs at the following point,

$$\alpha_0 = \frac{0.27216}{q}, \quad S = 6\pi q^2. \tag{36}$$

The existence of such an α_0 can be seen from **Figure 4**) as well (the extreme point at which only one solution for S exists, for a given value of α). Second, for any value beyond α_0, R is always positive, indicating the domination of repulsive interactions among microstructures, which overcome the attractive interactions intrinsic to the larger RN-AdS black holes. It will be seen that such a crossing can be explained by considering long range repulsive interactions to be associated with quintessence.

We now consider the $q = 0$ limit where the system is a Schwarzschild-AdS black hole surrounded by quintessence. As seen from the $q = 0$ limit of the Ruppeiner curvature in **Eq. 33**, quite remarkably, quintessence introduces a repulsion dominated region in the otherwise purely attractive Schwarzschild-AdS black hole. In this case one gets the crossing point of the Ruppeiner curvature to be simply at,

$$r_+ = \frac{1}{\alpha}, \tag{37}$$

or equivalently $\rho_0 = \alpha/2$ in terms of the density (defined as reciprocal of specific volume). Note that the crossing point increases with decrease in α, signifying the repulsive nature of the microstructures introduced due to quintessence. The Ruppeiner curvature is plotted as a function of r_+ in **Figure 5**.

There is another important novel consequence of the quintessence parameter α on the thermodynamic volume of Schwarzschild AdS black hole. In general in fluids, such as the vdW fluid, there is a

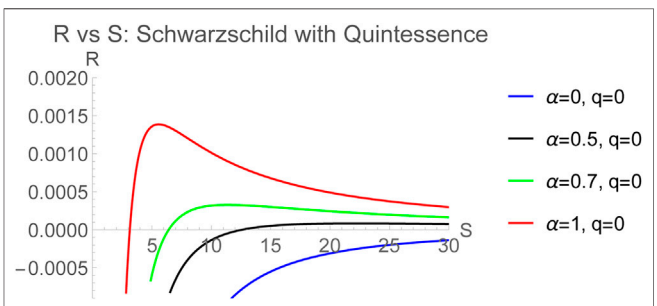

FIGURE 5 | Ruppeiner curvature for Schwarzschild-AdS black hole surrounded by quintessence on the (S, P)-plane as a function of S for fixed P.

[6]Indicating that the smaller black holes are dominated by repulsive interactions among microstructures [62,63]

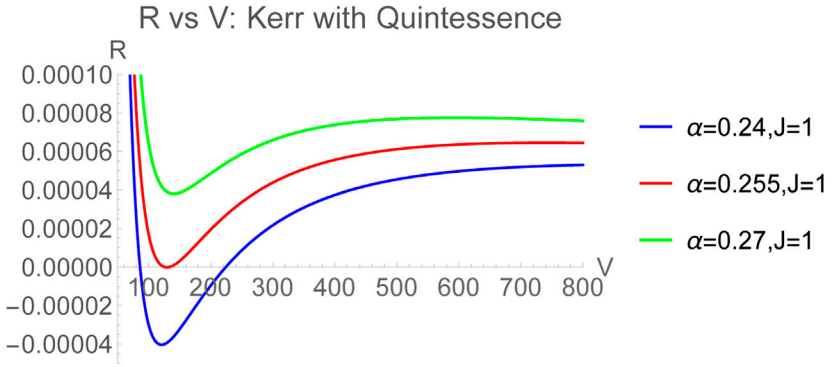

FIGURE 6 | Ruppeiner curvature for Kerr-AdS black hole surrounded by quintessence on the (T, V)-plane as a function of V for fixed T and angular momentum J.

minimum volume dictated by the fact that temperature does not become negative. This can be obtained from the equation of state evaluated at $T = 0$. Although Schwarzschild-AdS black holes do not show vdW behavior, in the presence of quintessence, there is a possibility of minimum volume given by,

$$V_{\min} = \frac{6\alpha^3 \pm \sqrt{\alpha^2 (36\pi P - 6\alpha^2)^2 - 1152\pi^3 P^3} - 36\pi\alpha P}{576\pi^2 P^3}. \quad (38)$$

It is clear that there is no minimum volume when $\alpha = 0$, corresponding the existence of only attractive interactions in the pure Schwarzschild-AdS (without quintessence) case [66].

3.2 Slowly Rotating Black Holes in AdS

The general expression for Ruppeiner curvature can be obtained analytically in the case $Q = 0$, $J \neq 0$, but complicated and not shown here. Instead, we plot the result directly, as shown in **Figure 6**. We find that behavior of R is qualitatively similar to the case of charged black holes in AdS, with J playing the role of Q. Therefore, even in present case, the presence of the quintessence parameter ensures that the Ruppeiner scalar has two zero crossings and hence one expects this to be a generic feature in other black hole systems too, including the case of a general rotating black hole.

Furthermore, there is a minimum volume dictated by the equation of state given in **Eq. 17** so that the temperature is not negative, which cannot be obtained analytically, but one can obtain its values numerically. For instance, considering the case $\alpha = 0.24$, the minimum volume is $V_{\min} = 3.08$. Keeping this in mind, even if there are additional points where R goes to zero below this volume, they are ignored as they are not physical from the point of view of the equation state.

4 MICROSTRUCTURES OF BLACK HOLES AND A MEAN FIELD DESCRIPTION

Analysis of Ruppeiner curvature of AdS black holes in last section, shows a subtle interplay between the attraction and repulsion dominated regimes, which heuristically suggests the presence of both attractive and repulsive interactions in the system, akin to the behavior of microstructures in a vdW fluid [62, 63]. Despite long standing efforts, the true nature of microscopic degrees of freedom of black holes are not known yet. Following Boltzmann's lines, "if you can heat it, it has microstructure," current studies have tried to obtain whatever valuable information from connection between thermodynamic and gravitation properties of black holes. The black hole chemistry paradigm [27, 28] has shown that charged black holes in AdS have a rich phase structure similar to vdW systems, suggesting a possible molecular kind of microstructure emerging from the degrees of freedom for black holes as well. However, the analysis of thermodynamic curvature shows that the behavior of microstructures of the two systems is not the same, with the case of black holes being more subtle [62, 63, 65, 68]. There are also proposals that a general interacting system can probably also be modeled as a binary mixture [65, 68] of both attractive and repulsive microstructures which share the degrees of freedom of the total entropy. Here, we take these issues forward and show that within a mean field approximation, the interactions can be described by an effective mean field interaction potential whose extremum points correspond to points where the Ruppeiner metric is flat. However, we particularly emphasize on the fact that any analysis in this spirit is phenomenological and is possible due to the resemblance of the thermodynamic structure of AdS black holes with that of hydrostatic systems such as the vdW fluid. Therefore, we shall be exploring a fluid-like description of black hole microstructures which may be thought of as being analogous to the molecules present in a fluid. Since $v = 2r_+$ corresponds to the specific (fluid) volume of the black hole, a number density $\rho = 1/v$ can be naturally associated with the system [80, 86, 87]. One can then alternatively write the equation of state [**Eq. 31**] in terms of this density as,

$$P = \rho T + \left(\frac{\alpha}{2\pi}\right)\rho - \left(\frac{1}{2\pi}\right)\rho^2 + \left(\frac{2q^2}{\pi}\right)\rho^4. \quad (39)$$

The first term, which depends on the temperature is clearly the kinetic energy density[7] whereas the remaining terms signify non-

[7]Indeed from the equipartition theorem, $E \sim T$ and one can see that the equation of state for the ideal gas, $P = \rho T$ equivalently implies $P \sim \rho E$ making it a kinetic energy density.

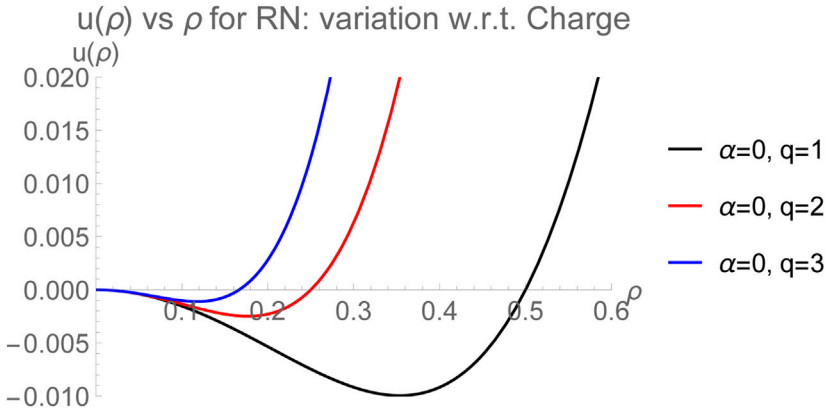

FIGURE 7 | Mean field interaction potential $u(\rho)$ as a function of ρ for various values of electric charge q with $\alpha = 0$.

trivial microscopic interactions. In fact, one can think of the remaining terms to correspond to a mean field potential energy density containing coarse grained information of the interactions and is given by,

$$u(\rho) = A\rho - B\rho^2 + C\rho^4, \tag{40}$$

where $A = \alpha/2\pi$, $B = 1/2\pi$ and $C = 2q^2/\pi$ are all positive constants. It is then expected that the extremum of such a mean field interaction potential would dictate the points of no effective interactions. This is indeed true and **Eq. 35** whose physical solutions correspond to the crossing points of the Ruppeiner curvature can alternatively be obtained as,

$$\left(\frac{\partial u}{\partial \rho}\right) = 0. \tag{41}$$

In the following subsection, we demonstrate the utility of the mean field interaction potential approach, by considering the special case $\alpha = 0$, i.e., RN-AdS black holes in the absence of quintessence. The cases with non-trivial dependence on quintessence are discussed in the next subsection.

4.1 RN-AdS Black Holes

For the case of RN-AdS black holes without quintessence in the background, the mean field interaction potential is given as,

$$u(\rho) = -\left(\frac{1}{2\pi}\right)\rho^2 + \left(\frac{2q^2}{\pi}\right)\rho^4, \tag{42}$$

and is plotted as a function of ρ for various values of the electric charge q in **Figure 7**.

In all the cases, there exists a minimum[8] of the potential where the attractive and repulsive interactions balance out. This point corresponds to $\rho_0 = \sqrt{1/8q^2}$ reproducing the previously known result for the horizon radius, $r_+ = \sqrt{2}|q|$ [68]. The first derivative of $u(\rho)$ is positive for $\rho > \rho_0$ whereas it is negative for $\rho < \rho_0$, translating respectively to repulsion and attraction dominance. This goes well with previously known conclusions for RN-AdS black holes where there exists a long range attraction and a short range repulsion [62]: ρ_0 represents the density at which the repulsion and attraction balance out whereas compressing the fluid to a smaller volume and hence, greater density leads to dominance of repulsion and vice versa. Moreover, since for a fluid[9], the density scales as $\rho \sim r^{-3}$ where r is a length scale typically of order of the mean free path of the molecules[10], the form of the mean field interaction potential [**Eq. 42**] suggests toward an intermolecular interaction of the Lennard-Jones type[11] as pointed out in [63,88],

$$V(r) = -\frac{c}{r^6} + \frac{d}{r^{12}}, \tag{43}$$

where c and d are appropriate positive constants. The mean field approach is therefore consistent with the previously known results for RN-AdS black holes and provides a satisfactory picture of interactions among microstructures.

4.2 Effect of Dark Energy on the Mean Field Interaction Potential

We shall now consider the effect of quintessence on the microstructures of AdS black holes. The mean field interaction potential in this case takes the form,

[8]Since $\rho = 0$ (or equivalently $v = \infty$) is not physical, the only physical point at which this mean field interaction potential admits an extremum is the minimum.

[9]The fluid in our discussions always assumes three spatial dimensions, irrespective of the number of spacetime dimensions in which the black hole (whose thermodynamics gets mapped into that of the fluid) resides in.

[10]With the assumption that the fluid density is spatially uniform, without any loss of generality one can consider some arbitrarily small length scale r of the order of the mean free path of the molecules such that in a volume $v \sim r^3$, the number of fluid molecules is constant.

[11]See [85] for a deeper connection between zero crossings of Ruppeiner curvature and intermolecular interactions involving Lennard-Jones type potentials in a different context.

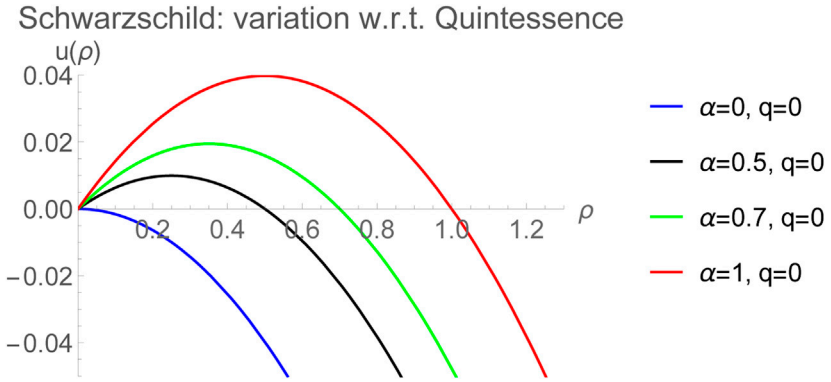

FIGURE 8 | Mean field interaction potential $u(\rho)$ as a function of ρ for various values of α with $q = 0$.

$$u(\rho) = \left(\frac{\alpha}{2\pi}\right)\rho - \left(\frac{1}{2\pi}\right)\rho^2. \tag{44}$$

Interestingly, the crossing point of the Ruppeiner curvature corresponds to a maximum, i.e., an unstable equilibrium of the mean field interaction potential,

$$\frac{\partial^2 u}{\partial \rho^2} = -\frac{1}{\pi}. \tag{45}$$

A plot of the mean field interaction potential is shown in **Figure 8**. This means that with ρ_0 being the value of the density at which attraction and repulsion balance out each other, a higher density would mean attraction dominance while a lower density would imply the dominance of repulsion: a conclusion which is completely opposite from that from the pure RN-AdS case discussed in the previous subsection. A fluid such as this one would admit a microscopic intermolecular potential whose repulsive part has a range which is longer than that of the attractive part. By our arguments from the previous subsection, it is suggestive from the form of **Eq. 44** that such a fluid would have a microscopic intermolecular potential of the form,

$$V(r) = \frac{b}{r^3} - \frac{c}{r^6}, \tag{46}$$

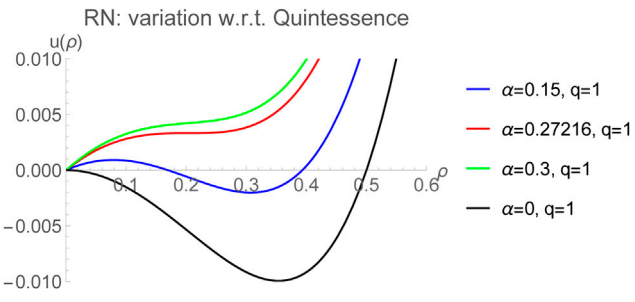

FIGURE 9 | Mean field interaction potential $u(\rho)$ as a function of ρ for various values of α with $q = 1$.

where b and c are both positive constants. The first and second terms respectively correspond to the repulsive and attractive parts of the intermolecular interaction. Naively, such an observation looks bizarre, but can be explained from the fact that quintessence, which corresponds to a negative pressure responsible for the expansion of the Universe is essentially a long ranged repulsive interaction with a range that is naturally longer than the range of attractive interactions between microstructures of the Schwarzschild-AdS black hole. Microstructures associated with quintessence are therefore not just repulsive, but have long ranged interactions, which typically go as an inverse cube of the distance.

The presence of a non-trivial electric charge makes the behaviour of the mean field interaction potential all the more interesting and is shown in **Figure 9**.

Note that the black curve corresponds to the RN-AdS case without quintessence, i.e., $\alpha = 0$. The red one corresponds to $\alpha = \alpha_0 = 0.27216$ (with $q = 1$) and one can see that for $\alpha > \alpha_0$ (the green curve), there are no extremum points of $u(\rho)$ indicating absence of zero crossings of the Ruppeiner curvature. In fact, for this case, the first derivative of the mean field interaction potential is positive definite. Such a situation dictates complete absence of attraction dominance from the system and the Ruppeiner curvature is wholly positive. The case with $\alpha < \alpha_0$ (the blue curve) is the most interesting one where there are two extremum points now as compared to the previous cases with zero crossings where there was either a maximum or a minimum. This means that there are now two equilibrium points where the net interactions balance out. Let us say these points correspond to the values ρ_{01} and ρ_{02} with $\rho_{01} < \rho_{02}$. At ρ_{01}, the equilibrium is an unstable one, meaning that further compression of the fluid would lead to attraction rather than repulsion and vice versa. It is around this unstable equilibrium that the third term of **Eq. 40** has little consequence[12] and equilibrium is reached primarily as

[12]The presence of electric charge would of course shift the position of this maximum but does not change the qualitative behavior of $u(\rho)$ around the maximum.

balance of interactions which the first and second terms of **Eq. 40** signify. This is similar to the case of the neutral Schwarzschild-AdS black hole surrounded by quintessence. The other equilibrium point, which exists only if we consider non-trivial charge is a minimum at ρ_{02} and is hence stable. This equilibrium is reached primarily from a balance of interactions due to the second and third terms in **Eq. 40** while the first term has very little to do with the behavior of this minimum.

In this paper, we restricted to the special case where the quintessence equation of state parameter took the value $\omega_q = -2/3$. If instead, one would choose other values of ω_q, the quintessence dependent term appearing in the mean field interaction potential would get altered in the power of ρ (which is linear in the present case, see **Eq. 40**) changing the overall shape of $u(\rho)$ and hence the location of the zeros of the Ruppeiner curvature discussed in this work. Such cases might be interesting to pursue in the future, although for the form of geometry in **Eq. 4** and equation of state considered in this paper, it would imply that it is always associated with short ranged repulsive interactions. Therefore, apart from changes in the locations at which the potential shows extremum, the general conclusions obtained from the present work should remain unaltered even if calculations are done with other values of ω_q in that specified range.

5 REMARKS

In this work, we have focused on probing the nature of interactions among the microstructures for asymptotically AdS black holes surrounded by quintessence using methods of thermodynamic geometry. From the empirical behavior of thermodynamic scalar R, charged black holes in $d \geq 4$ are associated with both attraction and repulsion dominated regions [62, 63, 68]. In this paper we considered various limiting case of the equation of state in [37] and studied the effect of dark energy on thermodynamic geometry and microstructures of neutral, charged and slowly rotating black holes. It may be possible to phenomenologically model the black hole microstructures as composed of two distinct kinds from a fluid perspective, where there is an exact analogy of black hole system with vdW system [24, 63, 65, 68]. It is known from earlier studies that the repulsive interactions are rather short ranged as compared to their attractive counterparts, such that the overall microscopic interaction potential is suggestively of the Lennard-Jonnes type [63, 88]. Following on these ideas, we developed an effective mean field potential approach for a generic black hole system in AdS in **Section 4**, such that the details of regions of domination of interactions among microstructures correspond to the equilibrium points of this potential. We also learn that quintessence leads to long ranged repulsive effects. In extended thermodynamics, where the fluid analogy of the black hole system is well established [24, 30, 32], we see that the repulsive interaction due to quintessence is analogous to an inverse cube microscopic interaction among the fluid molecules,

$$V_{quint}(r) \sim \frac{1}{r^3}. \tag{47}$$

It would be interesting to see the effects of quintessence on the microstructures for black holes in higher derivative theories such as Gauss-Bonnet-AdS black holes or even the more general Lovelock-AdS and pure Lovelock-AdS black holes, leading to a complete classification of attraction and repulsion dominated regions for wide variety of black holes. Another important avenue for future work is to include thermal fluctuations, as it is known that fluctuations give additional contributions and modify the points where the Ruppeiner scalar R goes to zero. The effect of statistical fluctuations on thermodynamics and phase transitions is well studied and is known to change the definitions of entropy and free energy, with particularly novel consequences for large black holes [37, 89–94]. Thus, it should be intriguing to consider additional effects due to thermal fluctuations on the thermodynamic geometry of black holes with quintessence studied in this work.

DATA AVAILABILITY STATEMENT

The original contributions presented in the study are included in the article/**Supplementary Material**, further inquiries can be directed to the corresponding author.

AUTHOR CONTRIBUTIONS

All authors listed have made a substantial, direct, and intellectual contribution to the work and approved it for publication.

ACKNOWLEDGMENTS

A.S. wishes to thank the Council of Scientific and Industrial Research (CSIR), Government of India, for financial support. A.G. would like to acknowledge the financial support received from IIT Bhubaneswar in the form of an institute research fellowship. The authors are grateful to the anonymous referees for a careful reading of the manuscript and their useful comments which have led to an improvement of the article. C.B. would like to thank the Science and Engineering Research Board (SERB), Government of India, for financial support through the Mathematical Research Impact Centric Support (MATRICS) grant number MTR/2020/000135.

SUPPLEMENTARY MATERIAL

The Supplementary Material for this article can be found online at: https://www.frontiersin.org/articles/10.3389/fphy.2021.631471/full#supplementary-material.

REFERENCES

1. Riess AG, Filippenko AV, Challis P, Clocchiatti A, Diercks A, Garnavich PM, et al. Observational evidence from supernovae for an accelerating universe and a cosmological constant. *Astron J* (1998) 116:1009. doi:10.1086/300499
2. Perlmutter S, Aldering G, Goldhaber G, Knop RA, Nugent P, Castro PG, et al. Measurements of omega and lambda from 42 high redshift supernovae. *Astrophys J* (1999) 517:565. doi:10.1086/307221
3. Sahni V, Starobinsky AA. The case for a positive cosmological Λ-term. *Int J Mod Phys D* (2000) 9:373–444. doi:10.1142/s0218271800000542
4. Caldwell RR, Dave R, Steinhardt PJ. Cosmological imprint of an energy component with general equation of state. *Phys Rev Lett* (1998) 80:1582. doi:10.1103/physrevlett.80.1582
5. Chen S, Wang B, Su R. Hawking radiation in a d-dimensional static spherically-symmetric black Hole surrounded by quintessence. *Phys Rev D* (2008) 77:124011. doi:10.1103/physrevd.77.124011
6. Azreg-Aïnou M. Charged de Sitter-like black holes: quintessence-dependent enthalpy and new extreme solutions. *Eur Phys J C* (2015) 75(1):34. doi:10.1140/epjc/s10052-015-3258-3
7. Kiselev VV. Quintessence and black holes. *Class Quan Grav* (2003) 20:1187. doi:10.1088/0264-9381/20/6/310
8. Thomas BB, Saleh M, Kofane TC. Thermodynamics and phase transition of the Reissner-Nordström black hole surrounded by quintessence. *Gen Relativ Gravit* (2012) 44:2181–9. doi:10.1007/s10714-012-1382-z
9. Ghosh SG, Maharaj SD, Baboolal D, Lee T. Lovelock black holes surrounded by quintessence. *Eur Phys J C* (2018) 78(2):90. doi:10.1140/epjc/s10052-018-5570-1
10. Ghosh SG, Amir M, Maharaj SD. Quintessence background for 5D Einstein–Gauss–Bonnet black holes. *Eur Phys J C* (2017) 77(8):530. doi:10.1140/epjc/s10052-017-5099-8
11. Ghaderi K, Malakolkalami B. Effects of quintessence on thermodynamics of the black holes. *Astrophys Space Sci* (2016) 361(5):161. doi:10.1007/s10509-016-2744-x
12. Ghaderi K, Malakolkalami B. Thermodynamics of the Schwarzschild and the Reissner-Nordström black holes with quintessence. *Nucl Phys B* (2016) 903:10–8. doi:10.1016/j.nuclphysb.2015.11.019
13. Toledo JM, Bezerra VB. The Reissner–Nordström black hole surrounded by quintessence and a cloud of strings: thermodynamics and quasinormal modes. *Int J Mod Phys D* (2018) 28(1):1950023.
14. Chabab M, Iraoui S. Thermodynamic criticality of d-dimensional charged AdS black holes surrounded by quintessence with a cloud of strings background. *Gen Relat Gravit* (2020) 52:75. doi:10.1007/s10714-020-02729-4
15. Visser M. The Kiselev black hole is neither perfect fluid, nor is it quintessence. *Class. Quant Grav* (2020) 37:4. doi:10.1088/1361-6382/ab60b8
16. Cvetic M, Gibbons GW, Pope CN. Photon spheres and sonic horizons in black holes from supergravity and other theories. *Phys Rev D* (2016) 94:106005. doi:10.1103/PhysRevD.94.106005
17. Kastor D, Ray S, Traschen J. Enthalpy and the mechanics of AdS black holes. *Class Quan Grav* (2009) 26:195011. doi:10.1088/0264-9381/26/19/195011
18. Cvetic M, Gibbons G, Kubiznak D, Pope C. Black hole enthalpy and an entropy inequality for the thermodynamic volume. *Phys Rev D* (2011) 84:024037. doi:10.1103/PhysRevD.84.024037
19. Hawking SW, Page DN. Thermodynamics of black holes in anti-de sitter space. *Commun Math Phys* (1983) 87:577. doi:10.1007/bf01208266
20. Dolan BP. The cosmological constant and black-hole thermodynamic potentials. *Class Quan Grav* (2011) 28:125020. doi:10.1088/0264-9381/28/12/125020
21. Dolan BP. Pressure and volume in the first law of black hole thermodynamics. *Class Quan Grav* (2011) 28:235017. doi:10.1088/0264-9381/28/23/235017
22. Chamblin A, Emparan R, Johnson CV, Myers RC. Charged AdS black holes and catastrophic holography. *Phys Rev D* (1999) 60:064018. doi:10.1103/physrevd.60.064018
23. Chamblin A, Emparan R, Johnson CV, Myers RC. Holography, thermodynamics and fluctuations of charged AdS black holes. *Phys Rev D Bf* (1999) 60:104026. doi:10.1103/physrevd.60.104026
24. Kubiznak D, Mann RB. P-V criticality of charged AdS black holes. *J High Energ Phys* (2012) 07:033. doi:10.1007/JHEP07(2012)033
25. Cai RG, Cao LM, Li L, Yang RQ. P-V criticality in the extended phase space of Gauss-Bonnet black holes in AdS space. *J High Energ Phys* (2013) 09:005. doi:10.1007/JHEP09(2013)005
26. Caceres E, Nguyen PH, Pedraza JF. Holographic entanglement entropy and the extended phase structure of STU black holes. *JHEP* (2015) 09:184. doi:10.1007/JHEP09(2015)184
27. Karch A, Robinson B. Holographic black hole chemistry. *JHEP* (2015) 12:073. doi:10.1007/JHEP12(2015)073
28. Kubiznak D, Mann RB, Teo M. Black hole chemistry: thermodynamics with Lambda. *Class Quant Grav* (2017) 34(6):063001. doi:10.1088/1361-6382/aa5c69
29. Majhi BR, Samanta S. P-V criticality of AdS black holes in a general framework. *Phys Lett B* (2017) 773:203–7. doi:10.1016/j.physletb.2017.08.038
30. Gunasekaran S, Kubiznak D, Mann RB. Extended phase space thermodynamics for charged and rotating black holes and Born-Infeld vacuum polarization. *JHEP* (2012) 11:110. doi:10.1007/JHEP11(2012)110
31. Wei SW, Liu YX. Critical phenomena and thermodynamic geometry of charged Gauss-Bonnet AdS black holes. *Phys Rev D* (2013) 87:044014. doi:10.1103/physrevd.87.044014
32. Li GQ. Effects of dark energy on P-V criticality of charged AdS black holes. *Phys Lett B* (2014) 735:256–60. doi:10.1016/j.physletb.2014.06.047
33. Liu H, Meng X. Effects of dark energy on the efficiency of charged AdS black holes as heat engines. *Eur Phys J C* (2017) 77(8):556. doi:10.1140/epjc/s10052-017-5134-9
34. Guo XY, Li HF, Zhang LC, Zhao RContinuous Phase Transition and Microstructure of Charged AdS Black Hole with Quintessence. *Eur Phys J C* (2020) 80:168. doi:10.1140/epjc/s10052-019-7601-y
35. Wu Y, Xu W. Effect of dark energy on Hawking–page transition. *Phys Dark Univ* (2020) 27:100470. doi:10.1016/j.dark.2020.100470
36. Xu Z, Wang J. Kerr-Newman-AdS black hole in quintessential dark energy. *Phys Rev D* (2017) 95:064015. doi:10.1103/physrevd.95.064015
37. Sharif M, Ama-Tul-Mughani Q. Phase transition and thermal fluctuations of quintessential Kerr-Newman-AdS black hole. *Phys Dark Universe* (2020) 30:100723. doi:10.1016/j.dark.2020.100723
38. Bekenstein JD. Black holes and entropy. *Phys Rev D* (1973) 7:2333–46. doi:10.1103/physrevd.7.2333
39. Bekenstein JD. Generalized second law of thermodynamics in black-hole physics. *Phys Rev D* (1974) 9:3292–300. doi:10.1103/physrevd.9.3292
40. Hawking SW. Particle creation by black holes. *Commun.Math Phys.Commun Math Phys* (1975) 43:199–206. doi:10.1007/bf02345020
41. Hawking SW. Black holes and thermodynamics. *Phys Rev D* (1976) 13:191. doi:10.1103/physrevd.13.191
42. Bardeen JM, Carter B, Hawking SW. The Four laws of black hole mechanics. *Commun Math Phys* (1973) 31:161. doi:10.1007/bf01645742
43. Padmanabhan T. Equipartition of energy in the horizon degrees of freedom and the emergence of gravity. *Mod Phys Lett A* (2010) 25:1129. doi:10.1142/s021773231003313x
44. Cai RG, Cho JH. Thermodynamic curvature of the BTZ black hole. *Phys Rev D* (1999) 60:067502. doi:10.1103/physrevd.60.067502
45. Mirza B, Zamaninasab M. Ruppeiner geometry of RN black holes: flat or curved? *J High Energ Phys* (2007) 6:059. doi:10.1088/1126-6708/2007/06/059
46. Aman J, Bengtsson I, Pidokrajt N. Geometry of black hole thermodynamics. *Gen Relativity Gravitation* (2003) 35:1733. doi:10.1023/a:1026058111582
47. Shen JY, Cai RG, Wang B, Su RK. Thermodynamic geometry and critical behavior of black holes. *Int J Mod Phys A* (2007) 22:11. doi:10.1142/s0217751x07034064
48. Quevedo H, Sanchez A. Geometric description of BTZ black holes thermodynamics. *Phys Rev D* (2009) 79:024012. doi:10.1103/physrevd.79.024012
49. Sahay A, Sarkar T, Sengupta G. Thermodynamic geometry and phase transitions in Kerr-Newman-AdS black holes. *JHEP* (2010) 04:118. doi:10.1007/JHEP04(2010)118
50. Sahay A, Sarkar T, Sengupta G. On the thermodynamic geometry and critical phenomena of AdS black holes. *J High Energ Phys* (2010) 07:82. doi:10.1007/JHEP07(2010)082
51. Banerjee R, Ghosh S, Roychowdhury D. New type of phase transition in Reissner Nordström-AdS black hole and its thermodynamic geometry. *Phys Lett B* (2011) 696:156. doi:10.1016/j.physletb.2010.12.010
52. Niu C, Tian Y, Wu XN. Critical phenomena and thermodynamic geometry of Reissner-Nordström-anti-de Sitter black holes. *Phys Rev D* (2012) 85:024017. doi:10.1103/physrevd.85.024017
53. Mansoori SAH, Mirza B. Correspondence of phase transition points and singularities of thermodynamic geometry of black holes. *Eur Phys J C* (2014) 74:2681. doi:10.1140/epjc/s10052-013-2681-6

54. Quevedo H. Geometrothermodynamics of black holes. *Gen Relativ Gravit* (2008) 40:971. doi:10.1007/s10714-007-0586-0
55. Hendi SH, Panahiyan S, Eslam Panah B, Momennia M. A new approach toward geometrical concept of black hole thermodynamics. *Eur Phys J C* (2015) 75(10):507. doi:10.1140/epjc/s10052-015-3701-5
56. Dehyadegari A, Sheykhi A, Montakhab A. Critical behavior and microscopic structure of charged AdS black holes via an alternative phase space. *Phys Lett B* (2017) 768:235. doi:10.1016/j.physletb.2017.02.064
57. Bhattacharya K, Majhi BR. Thermogeometric description of the van der Waals like phase transition in AdS black holes. *Phys Rev D* (2017) 95(10):104024. doi:10.1103/PhysRevD.95.104024
58. Chabab M, Moumni HE, Iraoui S, Masmar K, Zhizeh S. More insight into microscopic properties of RN-AdS black hole surrounded by quintessence via an alternative extended phase space. *Int J Geom Methods Mod Phys* (2018) 15: 1850171. doi:10.1142/s0219887818501712
59. Kumara AN, Rizwan CA, Vaid D, Ajith K. Critical behaviour and microscopic structure of charged AdS black hole with a global monopole in extended and alternate phase spaces. *Gen. Relat. Quant. Cosmol.* (1906) 1906:11550, 1906. arXiv:1906.11550 [gr-qc].
60. Kumara AN, Rizwan CL, Hegde K, Ajith KM, Ali MS. Microstructure and continuous phase transition of a regular Hayward black hole in anti-de Sitter spacetime. *Gen Relat Quant Cosmol* (2003)2003:0889, 2003. arXiv:2003.00889 [gr-qc].
61. Kumara AN, Rizwan CLA, Hegde K, Ajith KM. Repulsive interactions in the microstructure of regular Hayward black hole in anti-de Sitter spacetime. *Phys Lett B* (2020) 807:135556. doi:10.1016/j.physletb.2020.135556
62. Wei SW, Liu YX, Mann RB. Repulsive interactions and universal properties of charged Antiâde Sitter black hole microstructures. *Phys Rev Lett* (2019) 123(7). doi:10.1103/physrevlett.123.071103
63. Wei SW, Liu YX, Mann RB. Ruppeiner geometry, phase transitions, and the microstructure of charged AdS black holes. *Phys Rev D* (2019) 100:124033. doi:10.1103/physrevd.100.124033
64. Zangeneh MK, Dehyadegari A, Sheykhi A. Insight into the microscopic structure of an AdS black hole from a thermodynamical phase transition. *Phys Rev Lett* (2015) 115:111302. doi:10.1103/PhysRevLett.115.111302
65. Guo XY, Li HF, Zhang LC, Zhao R. Microstructure and continuous phase transition of a Reissner-Nordström-AdS black hole. *Phys Rev D* (2019) 100: 064036. doi:10.1103/physrevd.100.064036
66. Xu ZM, Wu B, Yang WL. Ruppeiner thermodynamic geometry for the Schwarzschild-AdS black hole. *Phys Rev D* (2020) 101:024018. doi:10.1103/physrevd.101.024018
67. Wei SW, Liu YX. Intriguing microstructures of five-dimensional neutral Gauss-Bonnet AdS black hole. *Phys Lett B* (2020) 803:135287. doi:10.1016/j.physletb.2020.135287
68. Ghosh A, Bhamidipati C. Thermodynamic geometry for charged Gauss-Bonnet black holes in AdS spacetimes. *Phys Rev D* (2020) 101:046005. doi:10.1103/physrevd.101.046005
69. Zhou R, Liu YX, Wei SW. Phase transition and microstructures of five-dimensional charged Gauss-Bonnet-AdS black holes in the grand canonical ensemble. *Phys Rev D* (2008) 102:124015. doi:10.1103/PhysRevD.102.124015
70. Wei SW, Liu YX, Mann RB. Novel dual relation and constant in Hawking-Page phase transition. *Phys Rev D* (2020) 102:104011. doi:10.1103/PhysRevD.102.104011
71. Dehyadegari A, Sheykhi A, Wei SW. Microstructure of charged AdS black hole via P−V criticality. *Phys Rev D* (2020) 102(10):104013. doi:10.1103/PhysRevD.102.104013
72. Yerra PK, Bhamidipati C. Constancy of Ruppeiner curvature along a renormalization group flow (2007). arXiv:2007.11515 [hep-th].
73. Ghosh A, Bhamidipati C. Thermodynamic geometry and interacting microstructures of BTZ black holes. *Phys Rev D* (2020) 101:106007. doi:10.1103/physrevd.101.106007
74. Ruppeiner G. Thermodynamics: a Riemannian geometric model. *Phys Rev A* (1979) 20:1608. doi:10.1103/physreva.20.1608
75. Ruppeiner G. Application of Riemannian geometry to the thermodynamics of a simple fluctuating magnetic system. *Phys Rev A* (1981) 24:488. doi:10.1103/physreva.24.488
76. Janyszek H, Mrugala R. Riemannian geometry and the thermodynamics of model magnetic systems. *Phys Rev A Gen Phys* (1989) 39:6515. doi:10.1103/physreva.39.6515
77. Janyszek H. Riemannian geometry and stability of thermodynamical equilibrium systems. *J Phys A Math Gen* (1990) 23:477. doi:10.1088/0305-4470/23/4/017
78. Janyszek H, Mrugaa R. Riemannian geometry and stability of ideal quantum gases. *J Phys A: Math Gen* (1990) 23:467. doi:10.1088/0305-4470/23/4/016
79. Ruppeiner G. Riemannian geometry in thermodynamic fluctuation theory. *Rev Mod Phys Rev Mod Phys* (1996) 6768:605313. doi:10.1103/RevModPhys.67.605
80. Ruppeiner G. Thermodynamic curvature measures interactions. *Am J Phys* (2010) 78:1170. doi:10.1119/1.3459936
81. Ruppeiner G. Thermodynamic curvature from the critical point to the triple point. *Phys Rev E Stat Nonlin Soft Matter Phys* (2012) 86:021130. doi:10.1103/PhysRevE.86.021130
82. Weinhold F. Metric geometry of equilibrium thermodynamics. *The J Chem Physics J Chem Phys* (1975) 63:2479. doi:10.1063/1.431689
83. Newman E, Penrose R. An approach to gravitational radiation by a method of spin coefficients. *J Math Phys* (1962) 3(3):566–78. doi:10.1063/1.1724257
84. Hawking SW. The conservation of matter in general relativity. *Commun Math Phys* (1970) 18:301. doi:10.1007/bf01649448
85. May HO, Mausbach P, Ruppeiner G. Thermodynamic curvature for attractive and repulsive intermolecular forces. *Phys Rev E Stat Nonlin Soft Matter Phys* (2013) 88:032123. doi:10.1103/PhysRevE.88.032123
86. Wei SW, Liu YX. Insight into the microscopic structure of an AdS black hole from a thermodynamical phase transition. *Phys Rev Lett Phys Rev Lett* (2015) 115(16):111302. doi:10.1103/PhysRevLett.115.111302
87. Das Bairagya J, Pal K, Pal K, Sarkar T. The geometry of RN-AdS fluids. *Phys Lett B* (2020) 805:135416. doi:10.1016/j.physletb.2020.135416
88. Miao YG, Xu ZM. On thermal molecular potential among micromolecules in charged AdS black holes. *Phys Rev D* (2018) 98:044001. doi:10.1103/physrevd.98.044001
89. Pourhassan B, Faizal M, Debnath U. Effects of thermal fluctuations on the thermodynamics of modified Hayward black hole. *Eur Phys J C* (2016) 76:145. doi:10.1140/epjc/s10052-016-3998-8
90. Pourhassan B, Kokabi K, Rangyan S. Thermodynamics of higher dimensional black holes with higher order thermal fluctuations. *Gen Relativ Gravit* (2017) 49:144. doi:10.1007/s10714-017-2315-7
91. Sinha AK. Thermal fluctuations of stable quantum ADS Kerr-Newman black hole. *Gen Relat Quant Cosmol* (2016) 1608:08359, 2016. arXiv:1608.08359 [gr-qc].
92. Upadhyay S, Hendi SH, Panahiyan S, Panah BE. Thermal fluctuations of charged black holes in gravity's rainbow. *Prog Theor Exp Phys* (2018) 1809: 093E01, 2018. [arXiv:1809.01078 [gr-qc]].
93. Zhang M. Corrected thermodynamics and geometrothermodynamics for anti-de Sitter black hole. *Nucl Phys B* (2018) 935:170. doi:10.1016/j.nuclphysb.2018.08.010
94. Sharif M, Akhtar Z. Quasi-normal modes and thermal fluctuations of charged black hole with Weyl corrections. *Phys Dark Universe* (2020) 29:100589. doi:10.1016/j.dark.2020.100589

Conflict of Interest: The authors declare that the research was conducted in the absence of any commercial or financial relationships that could be construed as a potential conflict of interest.